Journal of Ceramic Processing Research. Vol. 23, No. 3, pp. 298~303 (2022)
(Received 1 November 2021, Received in revised form 13 December 2021, Accepted 10 January 2022)
https://doi.org/10.36410/jcpr.2022.23.3.298

J O U R N A L O F
Ceramic Processing Research

Wollastonite spin coating on zirconia substrate by sol-gel method

Hyunjung Park and Jong Kook Lee*
Department of Advanced Materials and Engineering, Chosun University, Gwangju 61452, Republic of Korea

A wollastonite coating layer was fabricated on a zirconia substrate via a sol-gel method to improve the bioactivity of 3Y-TZP—a bioinert material. Initially, the coated wollastonite surface possessed a porous microstructure; however, the coated area and film thickness increased proportionally with the increasing number of coating cycles. Furthermore, it was observed that dense and thin coating layers were formed on the zirconia substrate after one or two coating cycles; however, after three or four coating cycles, it was observed that porous and thick coating layers were formed on the zirconia substrate. The surface roughness depended on the thickness of the wollastonite coating layer, which increased with the increasing number of coating cycles. An *in vitro* test was conducted, wherein a wollastonite-coated specimen was immersed in a simulated body fluid solution for 14 days. The test results revealed that new hydroxyapatite particles precipitated and covered the surface of the wollastonite coating layer, thus confirming that the wollastonite coating layer significantly improved the bioactivity of zirconia, compared to the pure zirconia surface.

Keywords: Sol-gel coating, bioactive wollastonite, zirconia bioactivity.

Introduction

Yttria tetragonal zirconia polycrystals (Y-TZP) are considered a promising alternative for dental implants owing to their high strength and good long-term properties. Y-TZP is a bioinert and nonresorbable ceramic that exhibits excellent resistance to corrosion and wear, high flexural strength and fracture resistance, high translucency and radiopacity, low thermal conductivity, good biocompatibility, and esthetic characteristics. The color of original Y-TZP is ivory (color), which similar to that of natural teeth, and possesses similar light transmitting qualities [1-6].

It has been reported that zirconia is biocompatible; thus, reaction in tissues and direct bone apposition are significantly minimized [7-9]. Osteoblastic cells exhibit good proliferation and surface attachment to zirconia. However, despite their biocompatibility, zirconia implants are bioinert and cannot be used in medical implants with direct bone contact [10-11]. In bone repair and regeneration, bioactivity plays a crucial role in the selection of bioceramics [12-15]. The essential condition for a bone implant to bond to a living bone is the formation of a bone-like apatite layer on its surface [16, 17].

Therefore, it is necessary to improve the bioactivity of zirconia for wide application as an implant material. The bioactivity of ceramics is strongly dependent on their surface properties, such as surface composition and microstructural morphology.

Recently, the surface modification of zirconia implants by machining, sandblasting, and acid etching has been widely used to enhance surface bioactivity [18, 19]. However, surface finishing can cause operation failure of the zirconia implants due to a fracture by the surface flaws created during the surface treatments. An effective method to improve the bioactivity of zirconia is surface coating with bioactive materials, such as hydroxyapatite, tricalcium phosphate, and wollastonite ceramics [20, 21].

Wollastonite ceramics are promising bioactive materials for fabricating artificial bones owing to their excellent bioactivity and osteoconductivity. They have attracted considerable research interest as alternative low-cost bioceramics for medical applications, such as bone repair, tissue engineering, and drug delivery [22-24]. However, they have limited applications owing to their relatively high dissolution rate, which leads to lower bone bonding strength after implantation in the human body. Accordingly, they are expected to play an important role in reinforcing and improving the bioactive properties of bioinert ceramics used in bone composites [25-27]. For example, the fabrication of wollastonite coatings on bioinert zirconia leads to improved surface bioactivity and bone-binding ability [15, 28].

Wollastonite surface coatings can be applied to the bioactive surface modification of various dental or orthopedic implants at low temperatures [29]. Previous studies have reported that wollastonite ceramics exhibit high bioactivity and biodegradability. They can be used for bone repair and regeneration; moreover, they are well known to induce bone-like apatite particles in

*Corresponding author:
Tel : +82-230-7202
Fax: +82-232-2474
E-mail: jklee@chosun.ac.kr

physiological environments, and also facilitate ingrowth of hard tissues [30]. Several synthetic methods for the preparation of wollastonite powder and coating have improved the properties of bioceramics used for bone and dental implants [31]. Among them, the sol-gel method has been widely used as a simple method for preparing highly bioactive coatings of wollastonite [32]. In particular, spin coating in the sol-gel process is a simple and economical method for the surface modification of dental implants, resulting in a homogeneous film layer and easy surface coating of complex-shaped parts [33-36]. However, techniques for the control of sol composition and coating parameters are required to obtain good bioactivity and a highly roughened surface morphology. Hence, it is important to determine the mechanism of apatite formation on the surfaces of wollastonite coatings [37-39].

In this study, wollastonite sol-gel coating was applied to a zirconia substrate using a spin coater, and the resulting improvement in the surface bioactivity of the zirconia substrate was investigated. After observing the microstructural evolution and chemical composition of the wollastonite coating layer, we analyzed the effect of sol composition and number of coating cycles on the surface morphology of the wollastonite coating and the *in vitro* bioactivity in a simulated body fluid (SBF) solution. Finally, we evaluated the enhancement in the surface bioactivity of zirconia via wollastonite sol-gel coating.

Experimental Procedure

Materials and sol-gel coating

Disk-type zirconia substrates were fabricated via cold isostatic pressing under a pressure of 200 MPa for 10 min after uniaxial pressing using commercial 3 mol% Y_2O_3-stabilized zirconia (TZ-3Y, Tosoh Co.) powder. Dense 3Y-TZP substrates were obtained via sintering at 1450 ºC for 2 h. Tetraethyl orthosilicate (TEOS) and calcium nitrate tetrahydrate ($Ca(NO_3)_2 \cdot 4H_2O$) were employed as the sol precursors for the preparation of wollastonite sol. The two starting sol precursors were mixed in ethanol with the same molar ratio, because wollastonite is composed of SiO_2 and CaO in a molar ratio of 1:1. The optimal wollastonite sol composition was obtained from a preliminary experiment, with adequate viscosity for spin coating. First, 11.92 g of $Ca(NO_3)_2 \cdot 4H_2O$ was dissolved in 25 mL ethanol to control the concentration to 2 mol/L; subsequently, 11.36 mL of TEOS was dissolved with the same concentration. The two solutions were mixed using a magnetic stirrer for 24 h at room temperature 24 ºC.

Wollastonite coating on the 3Y-TZP substrate was performed via the sol-gel method using a spin coater. Five droplets of the wollastonite sol were added to the zirconia substrate via spinning, and rotation was performed for 60 s. The wollastonite-coated zirconia substrates were dried for 10 min at 70 ºC. The same coating cycles after drying were repeated two to four times to obtain a thick wollastonite coating layer. Finally, the wollastonite coating layers were heat-treated at 1350 ºC for 2 h in an electric furnace to obtain a dense coating layer and to increase the adhesion of the coating layer onto the substrate. The detailed experimental procedure is shown in Fig. 1.

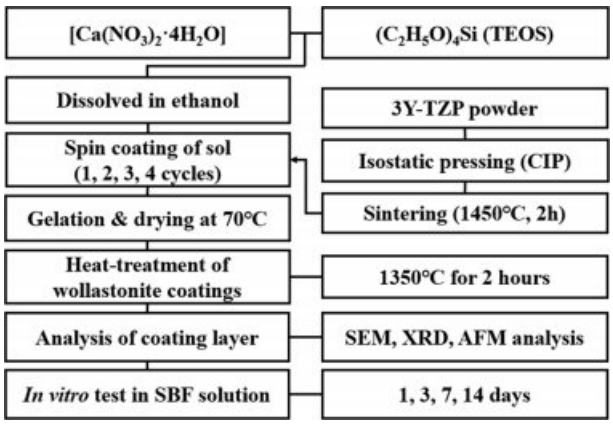

Fig. 1. Experimental procedure of the wollastonite coating process by sol-gel/spin method.

Characterization of coating layer and *in vitro* testing

The surface morphology and microstructure of the sintered 3Y-TZP substrate were observed using atomic force microscopy (AFM) and field-emission scanning electron microscopy (FE-SEM). The phase compositions of the zirconia substrate and wollastonite coating layers after heat treatment were analyzed using X-ray diffraction (XRD). The changes in the microstructural surface evolution and chemical composition of the wollastonite-coated surface with repeated coating cycles were analyzed using FE-SEM, energy-dispersive X-ray spectroscopy (EDS), and XRD. In addition, the surface morphology of the wollastonite-coated films was observed using AFM, and the surface roughness was evaluated with repeated coating cycles from the AFM photographs. The coating thickness was calculated from the perpendicular SEM photographs. Finally, the bioactivity of the wollastonite coating layer was confirmed via an *in vitro* test of a wollastonite-coated specimen by immersion in the SBF solution, placed in a thermostat at 36.5 ºC. After immersion for a maximum period of 14 days, the dissolution of wollastonite in the SBF solution and the precipitation of new apatite-like particles were investigated using SEM and XRD analysis; in addition, the improvement in the bioactivity of the zirconia substrate via wollastonite sol-gel/spin coating was investigated.

Results and Discussion

The phase composition, surface microstructure, and

morphology of the sintered zirconia substrates are shown in Fig. 2. The 3Y-TZP substrate has a dense and homogeneous microstructure with all tetragonal phases, a high sintered density of 6.03 g/cm^3, and a small grain size of less than 0.3 μm. The average surface roughness (Ra) of the 3Y-TZP substrate measured from the AFM photograph was 0.04 μm. The as-sintered specimen showed an uneven surface structure with several minimal cracks, which was expected to affect the deposition of wollastonite sol at the initial stage of sol-gel/spin coating.

Fig. 3 shows the microstructural changes of the wollastonite-coated surfaces on the zirconia substrate for different coating cycles. Unlike the zirconia substrate, all the wollastonite-coated surfaces fabricated via sol-gel/spin coating exhibited a highly roughened surface, regardless of the number of coating cycles. However, the amount of coated wollastonite particles, connectivity of wollastonite grains, and surface microstructure and roughness of the wollastonite coatings depended on the number of coating cycles. Scattered wollastonite islands were observed on the wollastonite-coated surface on the zirconia substrate fabricated with one coating cycle, and uncoated zirconia grains were simultaneously exposed on the surface of the wollastonite-coated specimen. With the increasing number of coating cycles, the connectivity of wollastonite particles on the coated surface increased, and numerous rounded pores were formed on the wollastonite-coated layer.

The perpendicular microstructure of the wollastonite coating layer on the zirconia substrate is shown in Fig. 4. The microstructure was strongly dependent on the number of coating cycles. All the wollastonite-coated layers were formed on zirconia substrates with uniform thickness, and they became thicker with repeated coating cycles. A thin and dense wollastonite-coated layer composed of small grains was formed after one coating cycle. In contrast, a thick and porous wollastonite-coated layer was obtained after four coating cycles, as shown in Fig. 4(d). Overall, the coating thickness and grain size of wollastonite gradually increased with the number of coating cycles, but the compactness between the grains in the wollastonite-coated layer decreased. It is suggested that the microstructural evolution with repeated coating cycles is related to the thermal decomposition of the wollastonite gel precursor [40]. After

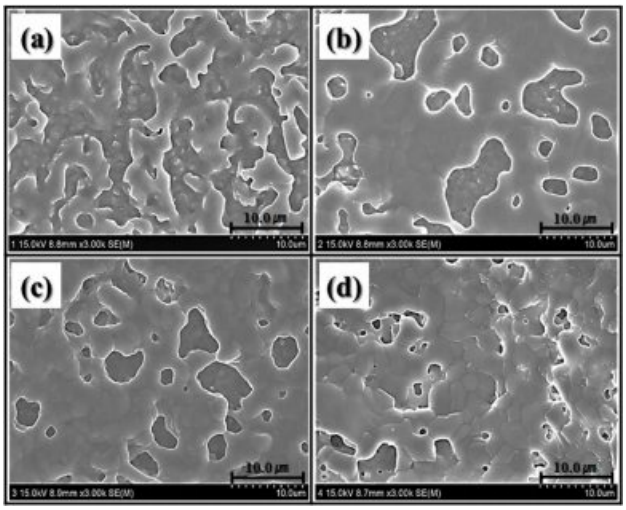

Fig. 3. Surface microstructure of wollastonite-coated layer with repeated coating cycle; (a) 1 cycle, (b) 2 cycles, (c) 3 cycles and (d) 4 cycles.

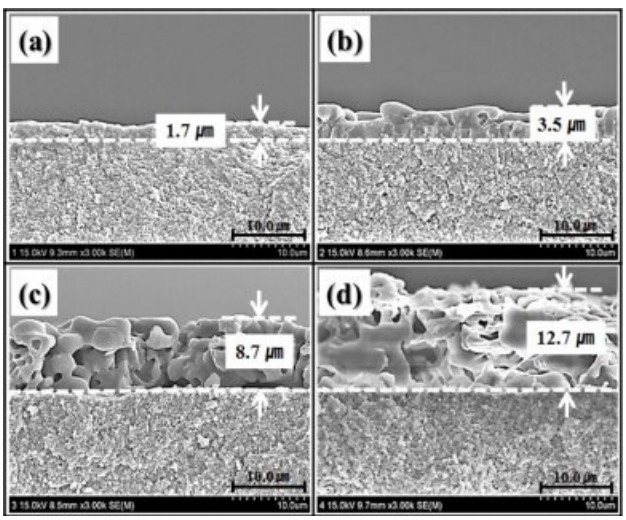

Fig. 4. Perpendicular microstructure of wollastonite-coated layer with repeated coating cycle; (a) 1 cycle, (b) 2 cycles, (c) 3 cycles and (d) 4 cycles.

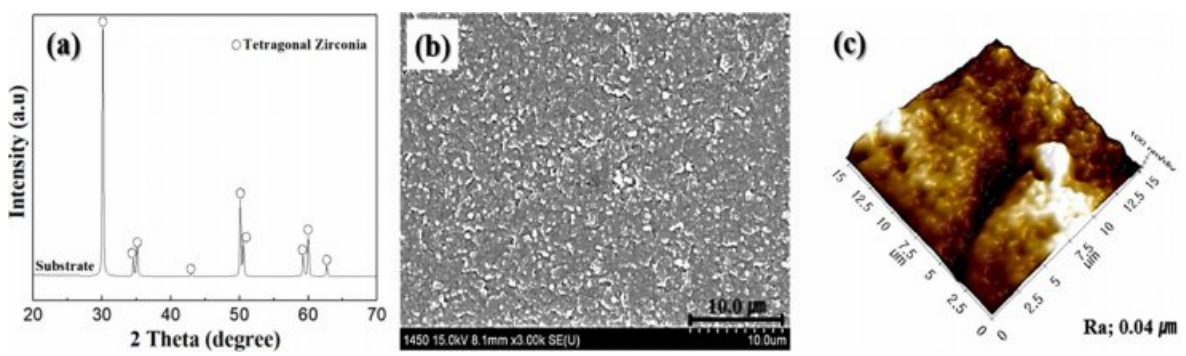

Fig. 2. Sintered characteristics of the 3Y-TZP substrate; (a) phase composition, (b) surface microstructure and (c) surface morphology.

the final heat treatment at 1350 °C for 2 h after drying the gel precursor, the gel precursor was thermally decomposed and transformed into wollastonite grains. At that time, several types of gas phases were formed within the coated layer via thermal decomposition, and they evaporated into the air while forming pores. Dense wollastonite-coated layer could be obtained from the thin gel precursor coating layer via rapid gas evaporation during the heat treatment. In contrast, thick coating layer formed by the gel precursor might have decomposed to form a porous microstructure via heat treatment at 1350 °C for 2 h. It is believed that thick wollastonite-coated layer with porous microstructure will have a positive effect on improving bioactivity, because it promotes the dissolution of the wollastonite coating layer in body, and then enhances apatite formation by releasing more calcium ions into the biological tissue [41].

Fig. 5 shows the surface morphology observed via AFM. A roughened surface morphology was formed by the wollastonite coating on zirconia, and it depended on the number of coating cycles. A highly roughened surface was obtained after four coating cycles with a thick coating layer with a porous microstructure. The variations in the coated layer thickness and surface roughness with the number of coating cycles are shown in Fig. 6. The wollastonite coating thickness on zirconia increased proportionally with increasing number of coating cycles from 1.7 μm to 12.7 μm. In addition, the surface roughness of the wollastonite-coated layer increased proportionally with the increasing number of coating cycles from 0.14 μm to 0.59 μm. Generally, a high surface roughness contributes to the improvement in bioactivity because it contributes to osteoconductivity and cell proliferation on the implant surface [42].

The phase composition of the wollastonite-coated 3Y-TZP substrate is shown in Fig. 7. Mixed peaks of tetragonal zirconia and α-wollastonite were observed on the surface of the wollastonite-coated 3Y-TZP substrate. With the thickening of the wollastonite-coated layer by repeated coating cycles, the intensity of the α-wollastonite peaks increased, whereas that of tetragonal zirconia decreased.

An *in vitro* test for the specimen with four coating cycles was conducted by immersing the wollastonite-coated specimen in the SBF solution for 14 days to examine the improvement in the bioactivity of zirconia via wollastonite coating. The morphological and phase changes were investigated using SEM and XRD analysis, respectively, as shown in Figs. 8 and 9. Clean surfaces of wollastonite particles were observed in the sample immersed for one day. Peaks of only α-wollastonite were observed, indicating that only surface dissolution of wollastonite occurred in the SBF solution during 1 day of immersion. However, after 3 days of immersion in the SBF solution, several new particles were precipitated on the surface of the wollastonite particles, which were confirmed be hydroxyapatite particles using XRD. In addition, as the immersion period was increased to 7 days, all the wollastonite surfaces were covered with small hydroxyapatite particles, which was confirmed via the increase in hydroxyapatite peaks, as observed from XRD analysis. After immersion for 14 days in the SBF solution, all the peaks of wollastonite disappeared in the XRD pattern and only hydroxyapatite peaks

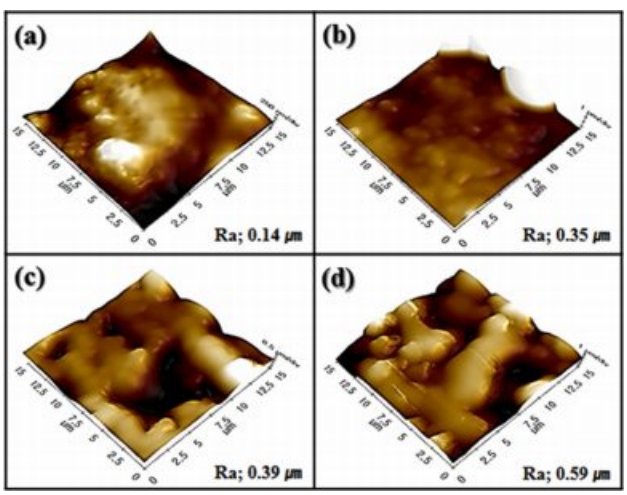

Fig. 5. Surface morphology and roughness of wollastonite-coated layer with repeated coating cycle; (a) 1 cycle, (b) 2 cycles, (c) 3 cycles and (b) 4 cycles.

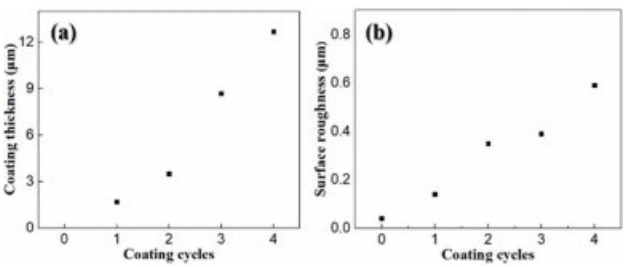

Fig. 6. Increment of (a) coating thickness and (b) surface roughness with repeated coating cycle.

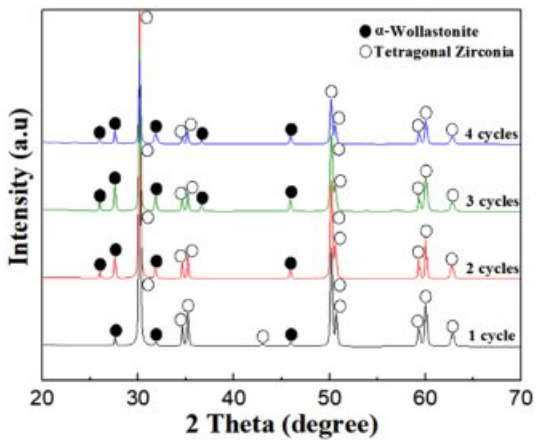

Fig. 7. Phase composition of wollastonite-coated zirconia substrate with repeated coating cycle.

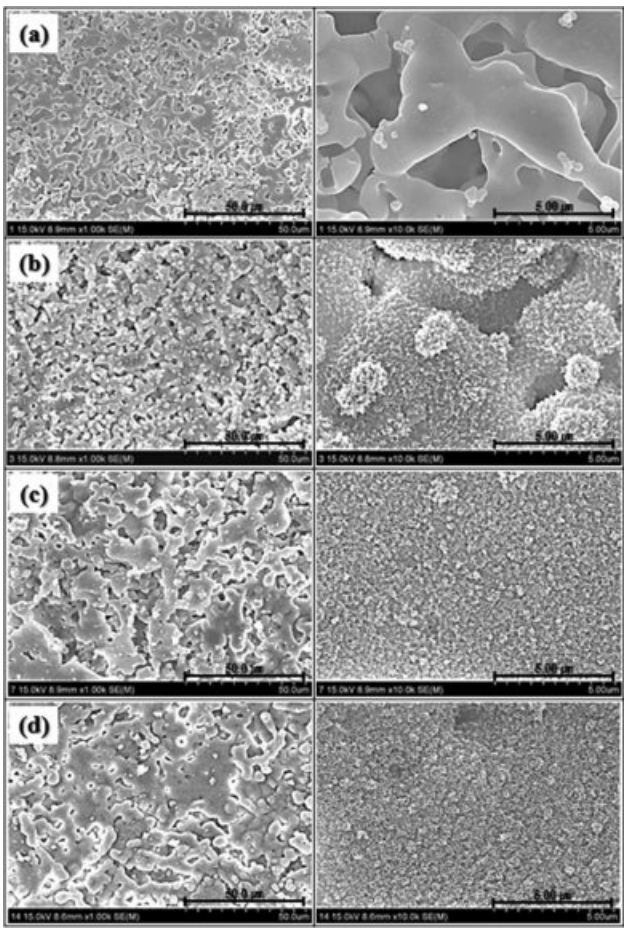

Fig. 8. Microstructural change of wollastonite-coated layer by *in vitro* test during the immersion into SBF solution; (a) 1 day, (b) 3 days, (c) 7 days and (d) 14 days.

were detected, suggesting the continuous dissolution of the wollastonite-coated layer and a rapid increase in the precipitated hydroxyapatite particles. The wollastonite sol-gel/spin coating plays an important role in the formation of a thick hydroxyapatite film on the zirconia substrate in the SBF solution. When bioactive ceramics are immersed in the SBF, ion-exchanges can take place between the ceramics and SBF, and finally the HA layers can be created on the surface of the ceramics. In general bioactivity of an artificial ceramics can be evaluated *in vitro* by examining the formation of apatite layer on its surface in SBF [43]. Apatite-forming ability of bioceramics is directly dependent on the chemical composition and dissolution, and wollastonite-based ceramics possess superior apatite-forming ability in SBF [44]. Thick wollastonite-coated layer on zirconia substrate fabricated by 4 repeated cycles may supply abundant Ca^{2+} ions by the release from coated surface into SBF solution during dissolution, and they induce the formation of crystallized apatite on substrate through forming an amorphous Ca-P deposition on the surface. Therefore, it was determined that thick wollastonite coating via the sol-gel/spin method effectively contributed to the improvement in the bioactivity of the bioinert zirconia substrate.

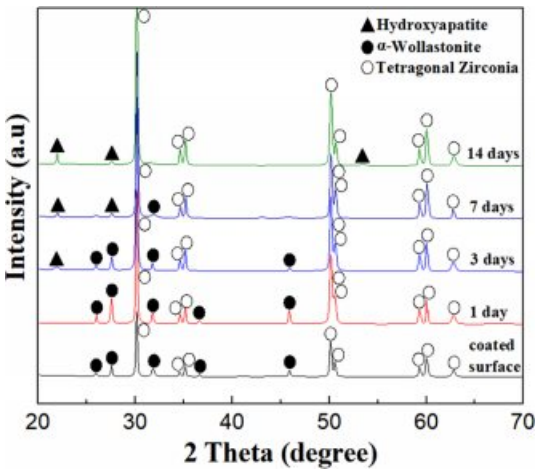

Fig. 9. Phase change of wollastonite-coated layer during the immersion from 1 to 14 days in SBF solution.

Conclusion

Homogeneous wollastonite layers were deposited on zirconia substrates via sol-gel/spin coating. The microstructure (dense or porous) of the wollastonite coating layer changed depending on the number of coating cycles and thickness of the coated layer. The wollastonite-coated area and film thickness increased proportionally with increasing number of coating cycles. In addition, the surface roughness (measured from AFM photographs) increased with increasing number of coating cycles and coating thickness. The *in vitro* test, wherein the wollastonite-coated specimen was immersed in the SBF solution, revealed that new precipitated hydroxyapatite particles were formed the surface of the wollastonite particles. The continuous dissolution of wollastonite particles and precipitation of hydroxyapatite particles were observed during immersion of the specimen in the SBF solution, and a thick hydroxyapatite film layer was finally formed on the zirconia substrate after 14 days of immersion. This confirmed that the wollastonite films formed via sol-gel/spin coating effectively improved the bioactivity of the zirconia substrate through the changes in microstructure, morphology, and chemical composition.

References

1. I. Denry, and J.A. Holloway, Materials. 3[1] (2010) 351-368.
2. E.S. Elshazly, S.M. El-Hout, and M.E.S. Ali, J. Mater. Sci. Technol. 27[4] (2011) 332-337.
3. M.J. Park, S.K. Yang, and J.B. Kang, J. Korean Ceram. Soc. 43[10] (2006) 640-645.
4. S.K. Hsu, H.C. Hsu, W.F. Ho, C.H. Yao, P.L. Chang, and S.C. Wu, Thin Solid Films. 572 (2014) 91-98.
5. P.F. Manicone, P.R. Iommetti, and L. Raffaelli, J. Dent. 35[11] (2007) 819-826.
6. H.J. Kim, J.J. Kim, and J.K. Lee, J. Nanosci. Nanotechnol.

19[10] (2019) 6285-6290.
7. I. Denry, and J.R. Kelly, Dent. Mater. 24[3] (2008) 299-307.
8. M. Andreiotelli, H.J. Wenz, and R.J. Kohal, Clin. Oral Implants Res. 20 (2009) 32-47.
9. H.B. Lim, D. Tang, K.J. Lee, and W.S. Cho, J. Korean Ceram. Soc. 48[2] (2011) 152-159.
10. M. Dehestani, L. Ilver, and E. Adolfsson, J. Biomed. Mater. Res. B. 100B[3] (2012) 832-840.
11. F.H. Schünemann, M.E. Galárraga-Vinueza, R. Magini, M. Fredel, F. Silva, J.C.M. Souza, Y. Zhang, and B. Henriques, Mater. Sci. Eng. C 98 (2019) 1294-1305.
12. C.A. Scotchford, C.P. Gilmore, E. Cooper, G.J. Leggett, and S. Downes, J. Biomed. Mater. Res. A 59[1] (2002) 84-99.
13. K. Anselme, Biomater 21[7] (2000) 667-681.
14. C. Gao, S. Peng, P. Feng, and C. Shuai, Bone. Res. 5 (2017) 17059-17092.
15. M. Demirel and B. Aksakal, J. Ceram. Process. Res. 19 (2018) 5-10.
16. A. Jemat, M.J. Ghazali, M. Razali, and Y. Otsuka, Biomed. Res. Int. 2015 (2015) 1-11.
17. J.W. Jeong, J.H. Kim, J.H. Shim, N.S. Hwang, and C.Y. Heo, Biomater. Res. 23[4] (2019) 1-11.
18. J. Li, P. Zhou, S. Attarilar, and H. Shi, Coatings. 11[6] (2021) 647-678.
19. L. Gaviria, J.P. Salcido, T. Guda, and J.L. Ong, J. Korean Assoc. Oral. Maxillofac. Surg. 40[2] (2014) 50-60.
20. M. Guazzato, M. Albakry, L. Quach, and M.V. Swain, Biomater 25[11] (2004) 2153-2160.
21. D. Arcos, and M. Vallet-Regi, J. Mater. Chem. B 8[9] (2020) 1781-1800.
22. R. Morsy, R. Abuelkhair, and T. Elnimr, Silicon. 9[4] (2017) 489-493.
23. F. Baino, G. Novajra, and C. Vitale-Brovarone, Front. Bioeng. Biotechnol. 3 (2015) 202-219.
24. B. Dhandayuthapani, Y. Yoshida, T. Maekawa, and D. Sakthi Kumar, Int. J. Polym. Sci. 2011 (2011) 1-19.
25. G. Brunello, H. Elsayed, and L. Biasetto, Materials. 12[18] (2019) 2929-2976.
26. G. Kaur, V. Kumar, F. Baino, J.C. Mauro, G. Pickrell, I. Evans, and O. Bretcanu, Mater. Sci. Eng. C 104 (2019) 109895-109909.
27. S.H. Ahn, D.S. Seo, and J.K. Lee, J. Ceram. Process. Res. 16 (2015) 548-554.
28. S. Sultana, M.M. Rahman, Z. Yeasmin, S. Ahmed and F.K. Rony, J. Ceram. Process. Res. 21 (2020) 285-295.
29. B. Priyadarshini, M. Rama, S. Chetan, and U. Vijayalakshmi, J. Asian Ceram. Soc. 7[4] (2019) 397-406.
30. M. Canillas, P. Pena, A.H. de Aza, and M.A. RodrÍguez, Bol. Soc. Esp. Ceram. Vidrio. 56[3] (2017) 91-112.
31. I.H.M. Aly, L.A.A. Mohammed, S. Al-Meer, K. Elsaid, and N.A.M. Barakat, Ceram. Int. 42[10] (2016) 11525-11534.
32. M. Mojahedian, F. Fahimipour, K.L. Larsen, M. Kalantar, F. Bastami and N. Omatli, J. Ceram. Process. Res. 17 (2016) 1138-1142.
33. E. Salahinejad, M.J. Hadianfard, D.D. Macdonald, M. Mozafari, D. Vashaee, and L. Tayebi, Mater. Lett. 97 (2013) 162-165.
34. J. Ballarre, R. Seltzer, E. Mendoza, J.C. Orellano, Y.W. Mai, C. GarcÍa, and S.M. Ceré, Mater. Sci. Eng. C 31[3] (2011) 545-552.
35. A. Barfeie, J. Wilson, and J. Rees, Br. Dent J. 218[5] (2015) E9-E18.
36. S. Vercaigne, J.G.C. Wolke, I. Naert, and J.A. Jansen, Clin. Oral. Impl. Res. 11[4] (2000) 314-324.
37. A. Milev, G.S.K. Kannangara, and B. Ben-Nissan, Mater. Lett. 57 (2003) 1960-1965.
38. N. Zhang, J.A. Molenda, S. Mankoci, X. Zhou, W.L. Murphy, and N. Sahai, Biomater. Sci. 1[10] (2013) 1101-1110.
39. C. Tatar, D. Bagci and O. Kaygili, J. Ceram. Process. Res. 17 (2016) 426-429.
40. D. Bellucci, A. Sola, R. Salvatori, A. Anesi, L. Chiarini, and V. Cannillo, Mater. Sci. Eng. C 43 (2014) 573-586.
41. C. Wu and J. Chang, Biomed. Mater. 8[3] (2013) 032001-03213
42. S. Kligman, Z. Ren, C.-H. Chung, M.A. Perillo, Y.-C. Chang, H. Koo, Z. Zheng, and C. Li, J. Clin. Med. 10[8] (2021) 1641-1677.
43. T. Miyazaki, J. Ceram. Soc. Jpn. 116[1350] (2008) 260-264.
44. A. Hoppe, N. S. Güldal and A.R. Boccaccini, Biomater. 32[11] (2011) 2757-2774.